

significance was calculated by using Mann–Whitney *U* test for comparison between 2 groups or by the Kruskal–Wallis test, followed by the Steel–Dwass test for multiple comparisons. Statistical analysis was performed with the Microsoft Excel software program with the add-in software Statcel3 (OMS, Japan). $P < 0.05$ was considered statistically significant.

Results

JAM-A Is Dominantly Secreted From CPCs

Previously, we have shown that the injection of CPCs reduces infarct size and restores cardiac function in comparison with the injection of BMs, SMs, and AMCs and that the beneficial effects are mediated not only by cardiomyogenesis but also by angiogenesis and antiapoptosis effects.⁴ This suggests that some of the humoral factors released from CPCs, but not from BMs, SMs, and AMCs, play an important role. When the quantity of secreted proteins from CPCs, BMs, SMs, and AMCs was measured by using a cytokine antibody array, CPCs secreted JAM-A, VCAM-1, and granulocyte-colony stimulating factor more than twice as much as did BMs, SMs, and AMCs (Table 2; total dataset presented in Table 3).

Soluble JAM-A Protein and CPC Conditioned Medium Prevent Transendothelial Migration of Neutrophils

Recently, it was reported that JAM-A is constitutively released from endothelial cells and epithelial cells via proteolytic shedding and inhibits neutrophil migration.⁶ Therefore, we examined whether CPC CM inhibits migration of neutrophils through HUVEC-coated transwell filters toward the chemoattractants. TNF α induced a significant increase in the number of transmigrated neutrophils in comparison with control (control, 6.7 ± 0.33 ; TNF α , 15 ± 1.8 ; Figure 2A). Preincubation of neutrophils with JAM-A Fc (4.7 ± 0.67) or CPC CM (3.3 ± 0.88) significantly inhibited transendothelial migration toward TNF α (Figure 2A). It has been reported that cardiomyocytes release neutrophil chemoattractant such as interleukin (IL)-8 under hypoxia.¹⁴ Hypoxia-exposed cardiomyocytes CM induced a significant increase in the number of transmigrated neutrophils in comparison with control (control, 7.7 ± 0.88 ; hypoxia CM, 27 ± 1.2 ; Figure 2B). Preincubation of neutrophils with JAM-A Fc (6.0 ± 0.58) or CPC CM (7.0 ± 1.2) significantly inhibited transendothelial migration stimulated by hypoxia-exposed cardiomyocyte CM (Figure 2B). When CPC CM was pretreated with neutralizing anti-JAM-A antibody, the inhibitory effect of CPC CM on neutrophil migration under the stimulation with TNF α and hypoxia-exposed cardiomyocyte CM was significantly attenuated (TNF α , 8.7 ± 0.33 ; Figure 2A: hypoxia CM, 13 ± 0.33 ; Figure 2B). This suggests that

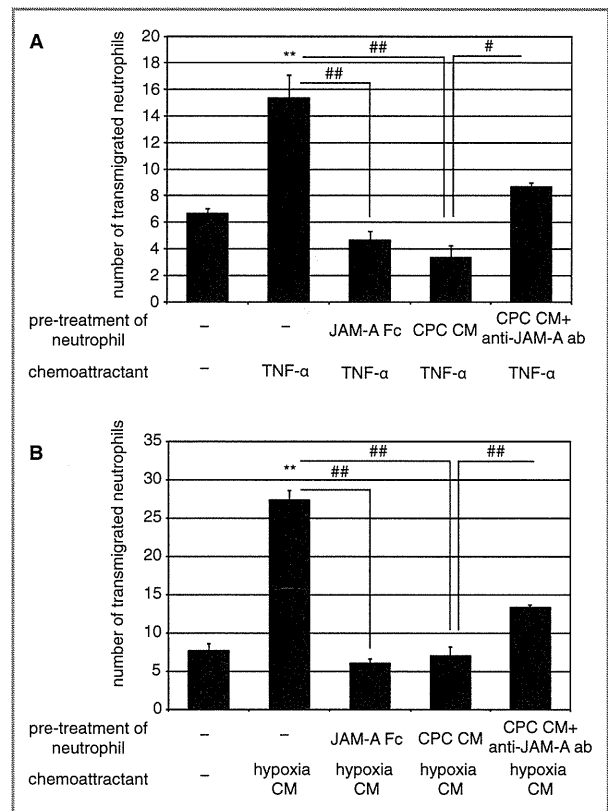


Figure 2. Soluble JAM-A and CPC CM inhibit transendothelial migration of neutrophils. Neutrophils were pretreated at 37°C for 10 minutes with JAM-A Fc (10 μ g/mL), CPC CM, or CPC CM with anti-JAM-A antibody (1 μ g/mL). Neutrophils were allowed to migrate across HUVECs in response to TNF α (A) or hypoxia-exposed cardiomyocytes CM (B) for 3 hours. Mean \pm SEM of 3 experiments. For statistical analysis, 1-way ANOVA–Tukey–Kramer post hoc test was performed. Significant differences between control and stimulated groups are shown by asterisks (** $P < 0.01$). Additional statistical comparisons are indicated by lines and number signs (## $P < 0.01$). CM indicates conditioned medium; CPC, cardiac progenitor cell; HUVEC, human umbilical vein endothelial cell; JAM-A, junctional adhesion molecule-A; TNF, tumor necrosis factor.

soluble form of JAM-A released from CPCs may play an important role in prevention of inflammatory response in ischemic myocardium through the inhibition of the extravasation of neutrophils.

Injection of CPCs Prevents Neutrophil Accumulation Through Secreted JAM-A

Next, we examined whether the injection of CPCs reduces accumulation of neutrophils after MI. Immunohistochemical images of the injured myocardium 1 day after MI revealed that fewer Ly6G-positive neutrophils were observed in

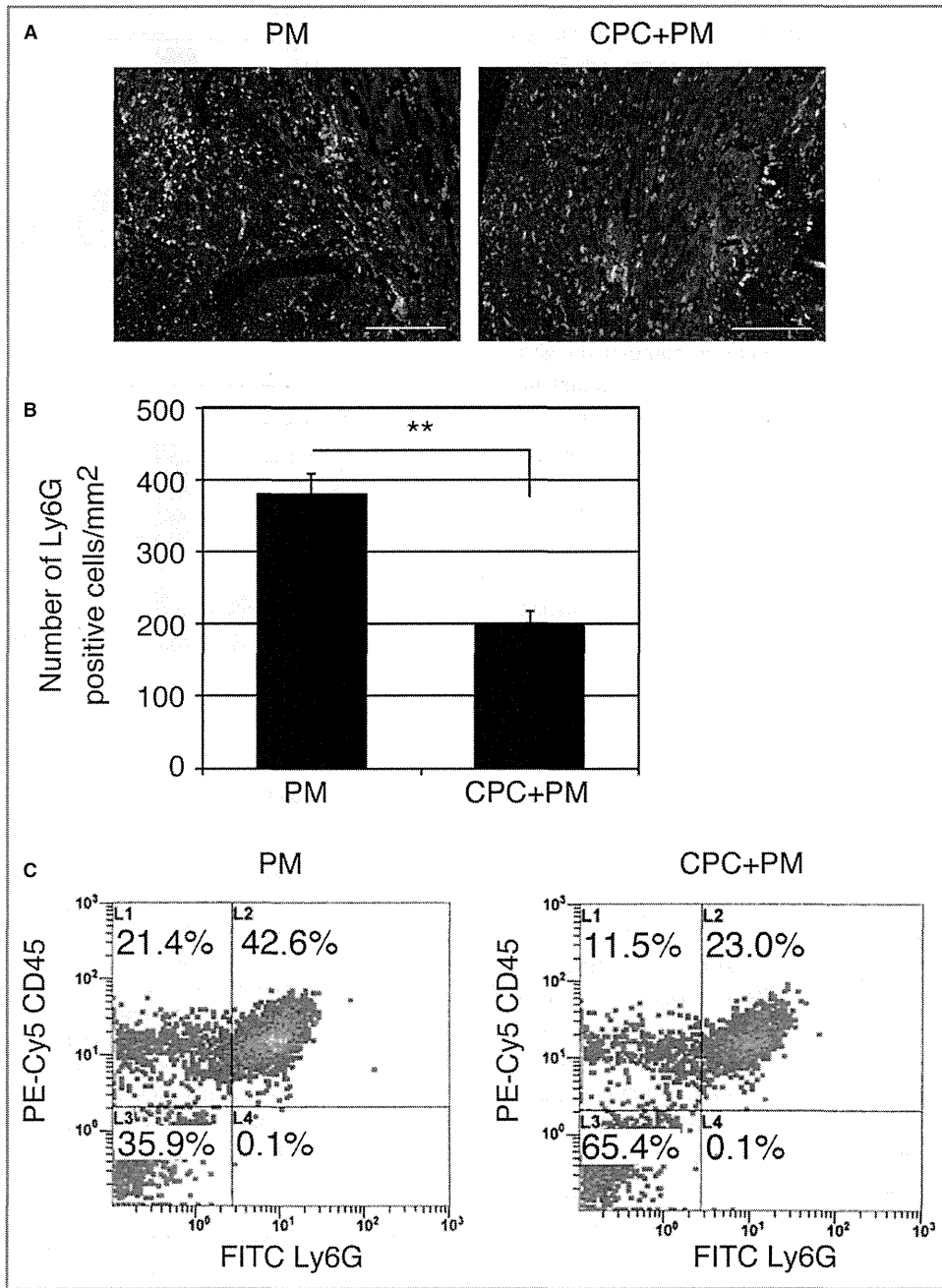


Figure 3. Injection of CPCs prevents neutrophil accumulation in ischemic myocardium. **A**, Immunohistochemical images of infarct area stained with anti-Ly6G antibody on 1 day after MI. Mouse was treated with PM or CPC+PM. Ly6G and nuclei are shown in green and blue, respectively. Morphology of tissue is shown in nonspecific green fluorescence. Bars were 0.2 mm. **B**, Quantification of neutrophil accumulation in the infarct area of PM- and CPC+PM-treated mice. To obtain the number of Ly6G-positive neutrophils/mm² in infarct area, 2 heart sections at papillary muscle level were examined per mouse. An average of values obtained from 3 mice for each group was presented. Asterisks denote statistical significant differences between PM- and CPC+PM-treated groups after Student *t* test (**P*<0.01). **C**, Representative dot plots from PM- or CPC+PM-treated MI hearts. Cell suspensions from PM- or CPC+PM-treated MI hearts were stained with anti-Ly-6G and anti-CD45 antibodies. Dot plots from a typical experiment of 2 performed are shown. CPC indicates cardiac progenitor cell; FITC, fluorescein isothiocyanate; MI, myocardial infarction.

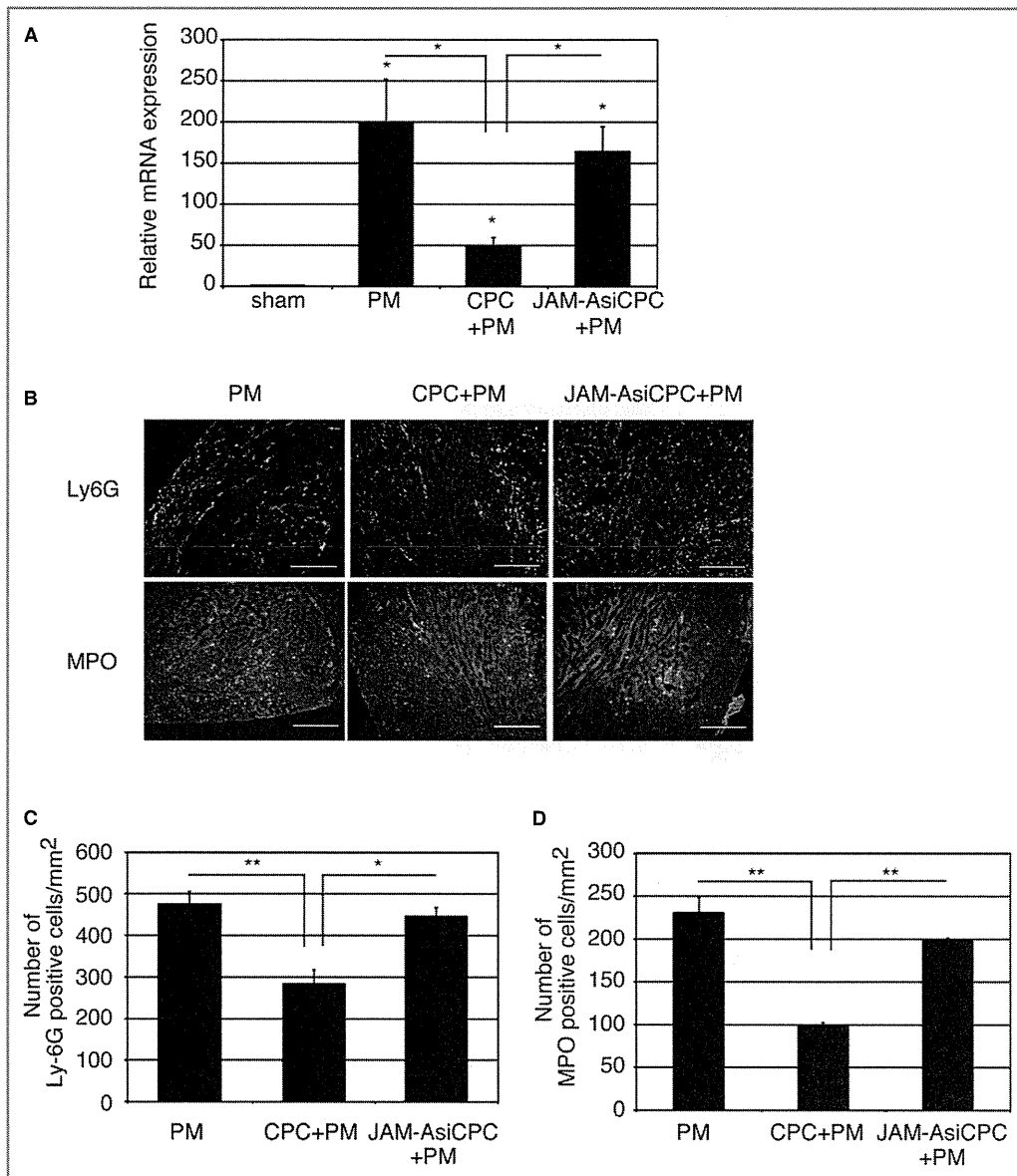


Figure 4. Knockdown of JAM-A attenuates CPC-mediated inhibitory effect on neutrophil accumulation. **A**, Transplantation of CPCs (CPC+PM) but not CPCs transfected with JAM-A siRNA (JAM-AsiCPC+PM) reduced relative expression level of *Ly6G* mRNA. RNA was extracted from left ventricle at 1 day after MI. Expression level was shown as fold changes relative to sham operated mouse using delta delta CT method: sham, n=6; PM, n=7; CPC+PM, n=6; JAM-AsiCPC+PM, n=5. The Kruskal–Wallis test, followed by the Steel–Dwass test was used for statistical analysis. Asterisks above individual columns indicate significant difference compared with sham. Asterisks above a line spanning 2 columns indicate significant difference between 2 groups ($*P<0.05$). **B**, Immunohistochemical images of infarct area stained with anti-Ly6G and anti-MPO antibodies at 1 day after MI. Mouse was treated with PM, CPC+PM, or JAM-AsiCPC+PM. Ly6G and MPO are shown in green and nuclei in blue. Morphology of tissue is shown in nonspecific green fluorescence. Bars were 0.2 mm. **C** and **D**, Quantification of neutrophil accumulation in the infarct area of PM-, CPC+PM-, and JAM-AsiCPC+PM-treated mice. To obtain the number of Ly6G (**C**) and that of MPO (**D**)-positive neutrophils/mm² in infarct area, 2 heart sections at papillary muscle level were examined per mouse. An average of values obtained from 3 mice for each group was presented. One-way ANOVA–Tukey–Kramer post hoc test was used for statistical analysis. Asterisks indicate statistical significant differences ($**P<0.01$ and $*P<0.05$). CPC indicates cardiac progenitor cell; JAM-A, junctional adhesion molecule-A; MI, myocardial infarction; MPO, myeloperoxidase; siRNA, small interfering RNA.

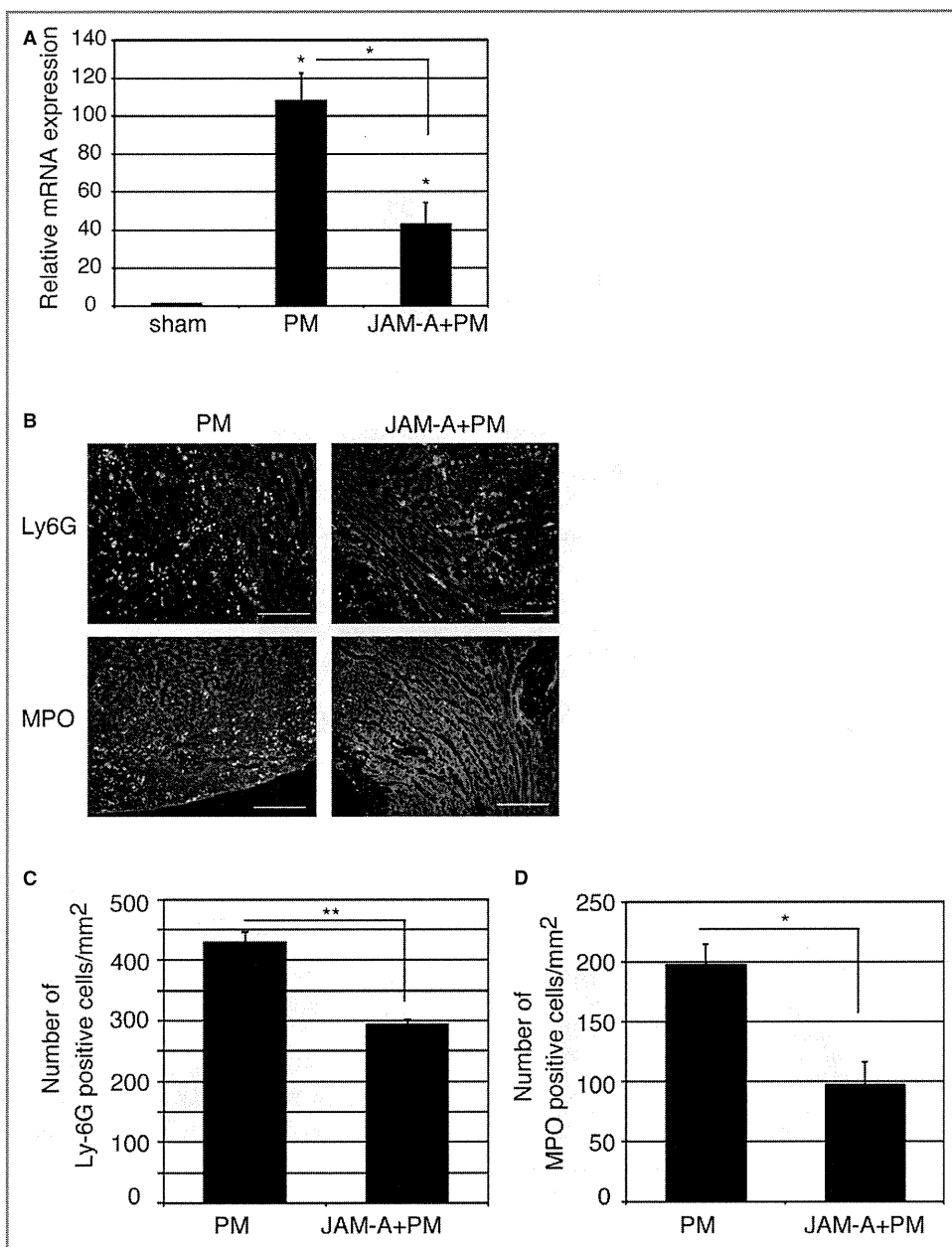


Figure 5. Injection of JAM-A Fc protein prevents neutrophil accumulation in ischemic myocardium. **A**, Transplantation of JAM-A Fc protein (JAM-A+PM) reduced relative expression level of *Ly6G* mRNA. RNA was extracted from left ventricle of day 1 MI heart. Expression level was shown as fold changes relative to sham operated mouse using delta delta CT method: sham, n=4; PM, n=5; JAM-A+PM, n=5. The Kruskal–Wallis test, followed by the Steel–Dwass test, was used for statistical analysis. Asterisks above individual columns indicate significant difference compared with sham. Asterisks above a line spanning 2 columns indicate significant difference between 2 groups (* P <0.05). **B**, Immunohistochemical images of infarct area stained with anti-Ly6G and anti-MPO antibodies at 1 day after MI. Mouse was treated with PM or JAM-A+PM. Ly6G and MPO are shown in green and nuclei in blue. Morphology of tissue is shown in nonspecific green fluorescence. Bars were 0.2 mm. **C** and **D**, To obtain the number of Ly6G (**C**) and that of MPO (**D**)-positive neutrophils/mm² in infarct area, 2 heart sections at papillary muscle level were examined per mouse. An average of values obtained from 3 mice for each group was presented. Student *t* test was used for statistical analysis. Asterisks indicate statistical significant differences (** P <0.01 and * P <0.05). JAM-A, junctional adhesion molecule-A; MI, myocardial infarction; MPO, myeloperoxidase.

CPC+PM-treated mice in comparison with PM-treated mice (Figure 3A). The number of Ly6G-positive neutrophils in the infarct area of CPC+PM-treated mice was significantly lower than that of PM-treated mice (PM: $378 \pm 29/\text{mm}^2$; CPC+PM: $202 \pm 16/\text{mm}^2$, $P < 0.01$, Figure 3B). Flow cytometric analysis revealed that percentages of CD45⁺Ly6G⁺ neutrophils of total live cells were decreased in CPC+PM-treated mice (23.0%) in comparison with PM-treated mice (42.6%) at 1 day after MI (Figure 3C).

We next examined whether CPC-derived JAM-A are involved in the prevention of neutrophil accumulation by RNA interference by using siRNA. We confirmed that siRNA selectively reduced the amount of JAM-A mRNA and secreted soluble JAM-A protein in CPCs (Figure 1A and 1B). When the expression levels of *Ly6G* gene was examined at 1 day after injection of PMs, CPCs+PMs, or CPCs transfected with JAM-A siRNA (JAM-AsiCPC)+PMs to MI heart, the expression levels of *Ly6G* were significantly reduced in CPC+PM-treated group in comparison with PM-treated group. The suppressive effect on *Ly6G* gene expression in the CPC+PM-treated group was abrogated when CPCs transfected with JAM-AsiCPC+PM was injected into MI hearts (PM: 198 ± 54.1 ; CPC+PM: 49.6 ± 9.27 ; JAM-AsiCPC+PM: 164 ± 30.2 , PM versus CPC+PM; $P < 0.05$, CPC+PM versus JAM-AsiCPC+PM; $P < 0.05$) (Figure 4A). Immunohistochemical images of the injured myocardium 1 day after MI showed that accumulation of Ly6G-positive neutrophils in PM-treated mice were prevented in CPC+PM-treated mice but not in JAM-AsiCPC+PM-treated mice (Figure 4B, upper row). Fewer MPO-positive neutrophils were observed in CPC+PM-treated mice in comparison with

PM-treated mice (Figure 4B, lower row). The reductive effect of CPC injection on the accumulation of MPO-positive neutrophils was attenuated in JAM-AsiCPC+PM-treated mice (Figure 4B, lower row). The number of Ly6G positive neutrophils in the infarct area was $474 \pm 31/\text{mm}^2$ in PM-treated, $284 \pm 33/\text{mm}^2$ in CPC+PM-treated, and $446 \pm 20/\text{mm}^2$ in JAM-AsiCPC+PM-treated mice (PM versus CPC+PM; $P < 0.01$, CPC+PM versus JAM-AsiCPC+PM; $P < 0.05$; Figure 4C). The number of MPO-positive neutrophils in the infarct area was $231 \pm 30/\text{mm}^2$ in PM-treated, $97.7 \pm 8.7/\text{mm}^2$ in CPC+PM-treated, and $197 \pm 6.4/\text{mm}^2$ in JAM-AsiCPC+PM-treated mice (PM versus CPC+PM; $P < 0.01$, CPC+PM versus JAM-AsiCPC+PM; $P < 0.01$; Figure 4D).

We then explored whether the injection of soluble JAM-A protein can inhibit accumulation of neutrophils in MI hearts. When a mixture of recombinant mouse JAM-A Fc protein and PM was injected into MI hearts, the expression levels of *Ly6G* were significantly reduced in JAM-A+PM-treated mice in comparison with PM-treated mice at 1 day after injection (PM: 108 ± 15 ; JAM-A+PM: 43.0 ± 12 , $P < 0.05$; Figure 5A). Immunohistochemical images of the injured myocardium 1 day after MI revealed that fewer Ly6G-positive neutrophils were observed in JAM-A+PM-treated mice in comparison with PM-treated mice (Figure 5B, upper row) and that fewer MPO-positive neutrophils were observed in JAM-A+PM-treated mice in comparison with PM-treated mice (Figure 5B, lower row). The number of Ly6G-positive neutrophils in the infarct area was $430 \pm 15/\text{mm}^2$ in PM-treated and $293 \pm 9.2/\text{mm}^2$ in JAM-A+PM-treated mice (PM versus JAM-A+PM; $P < 0.01$; Figure 5C). The number of MPO-positive neutrophils in the

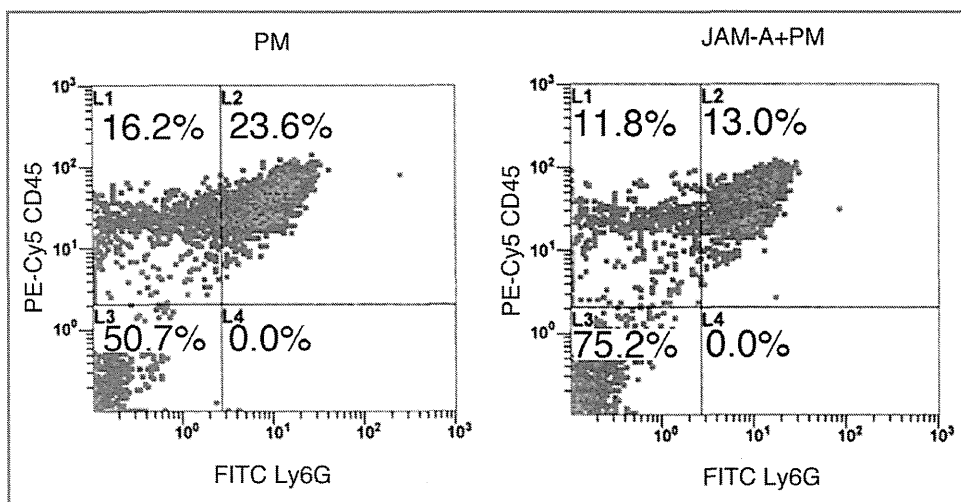


Figure 6. Injection of JAM-A+PM attenuates myocardial neutrophil infiltration after MI. Representative dot plots from PM- or JAM-A+PM-treated MI hearts. Cell suspensions from PM- or JAM-A+PM-treated MI hearts were stained with anti-Ly-6G and anti-CD45 antibodies. Dot plots from a typical experiment of 2 performed are shown. FITC indicates fluorescein isothiocyanate; JAM-A, junctional adhesion molecule-A; MI, myocardial infarction.

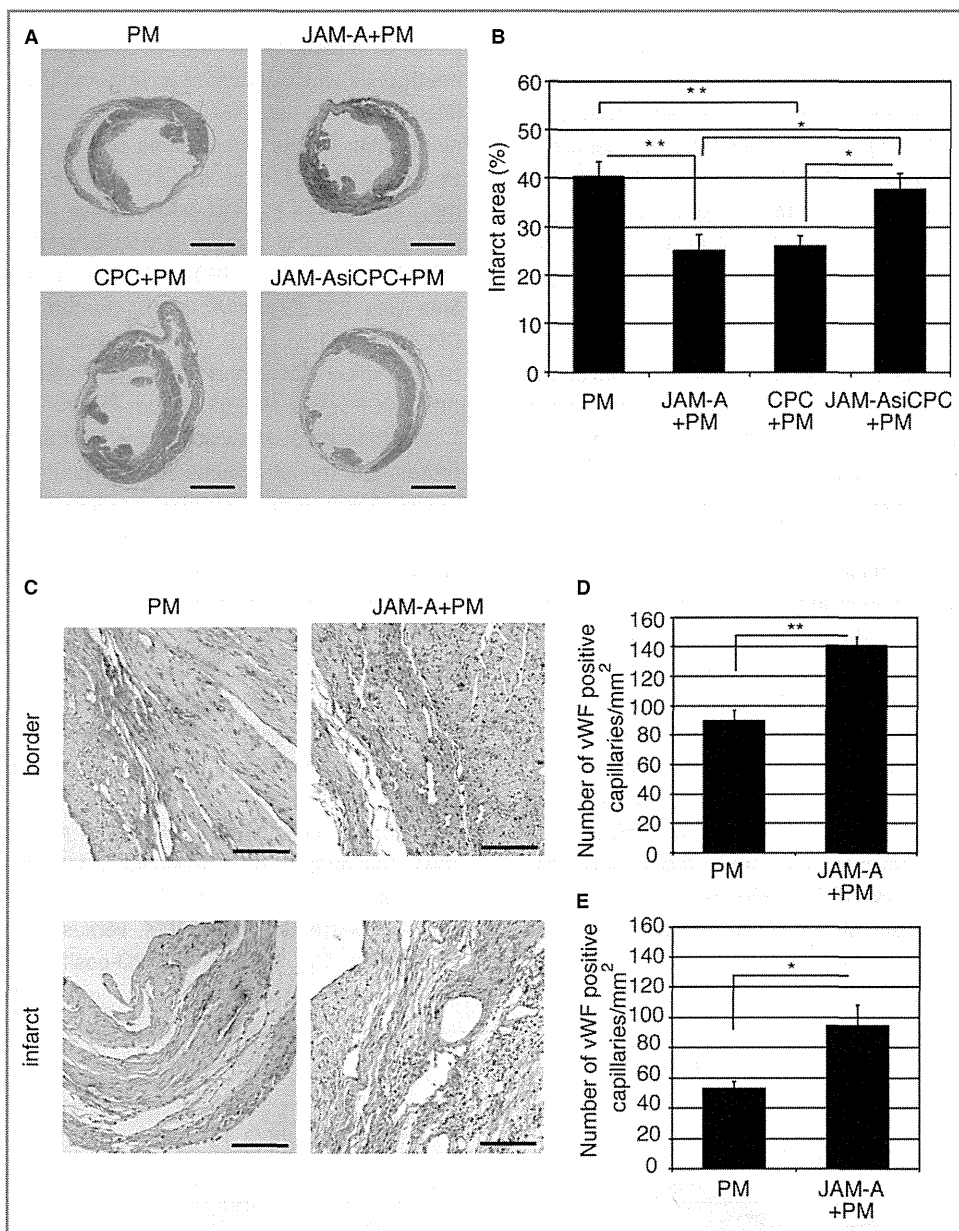


Figure 7. Soluble JAM-A mediates the reduction of infarct size and prevention of left ventricular remodeling, and enhances capillary density. **A**, Representative Masson’s trichrome–stained myocardial sections from PM-treated, JAM-A+PM–treated, CPC+PM–treated, and JAM-AsiCPC+PM–treated hearts. Bars are 2.5 mm. **B**, Quantification of infarct size 2 weeks after transplantation. For statistical analysis, 1-way ANOVA–Tukey–Kramer post hoc test was performed. Significant differences among groups are shown by asterisks (** $P < 0.01$ and * $P < 0.05$). **C**, Representative images from the sections of PM-treated and JAM-A+PM–treated hearts stained for capillaries with anti-vWF antibodies. Bars are 100 μ m. **D** and **E**, Quantification of the number of vWF–positive capillaries in border (**D**) and infarct (**E**) area 2 weeks after transplantation. To obtain the number of vWF–positive capillaries/mm² in infarct area and border area, 2 heart sections at papillary muscle level were examined per mouse. An average of values obtained from 3 mice for each group was presented. Student *t* test was used for statistical analysis. Asterisks indicate statistical significant differences (** $P < 0.01$ and * $P < 0.05$). JAM-A indicates junctional adhesion molecule-A; vWF, von Willebrand factor.

Table 4. Echocardiographic Measurement of Hearts 2 Weeks After Transplantation

Parameter	n	HR, beats/min	SWT, mm	PWT, mm	LVIDD, mm	LVISD, mm	%FS
PM	9	672±13	0.27±0.05	0.30±0.04	6.2±0.20	5.8±0.26	6.9±1.3
JAM-A+PM	11	711±11	0.43±0.05 ^{††}	0.52±0.05 ^{**††}	4.9±0.32 [*]	4.2±0.37 [*]	15±2.0 ^{*†}
CPC+PM	9	683±20	0.43±0.08 [†]	0.57±0.04 ^{**††}	4.9±0.24 ^{**}	4.1±0.27 ^{**†}	15±2.4 ^{*†}
JAMAsiCPC+PM	7	708±11	0.15±0.02	0.22±0.05	6.2±0.34	5.8±0.40	6.9±1.4

Statistical analysis was performed by 1-way ANOVA–Tukey–Kramer post hoc test (HR, PWT, and %FS) or Kruskal–Wallis test, followed by Steel–Dwass test (SWT, LVIDD, and LVISD). CPC indicates cardiac progenitor cell; FS, fractional shortening; HR, heart rate; JAMA, junctional adhesion molecule-A; LVIDD, left ventricular internal diastolic diameter; LVISD, left ventricular internal systolic diameter; PWT, posterior wall thickness; siCPC, CPC transfected with JAM-A silent interfering RNA; SWT, septal wall thickness.

* $P<0.05$ vs PM, ** $P<0.01$ vs PM, [†] $P<0.05$ vs JAM-AsiCPC+PM, ^{††} $P<0.01$ vs JAM-AsiCPC+PM.

infarct area was $197\pm 18/\text{mm}^2$ in PM-treated and $96.8\pm 20/\text{mm}^2$ in JAM-A+PM-treated mice (PM versus JAM-A+PM; $P<0.01$; Figure 5D). Flow cytometric analysis revealed that percentages of CD45⁺Ly6G⁺ neutrophils of total live cells decreased in JAM-A+PM-treated mice (13.0%) in comparison with PM-treated mice (23.6%) at 1 day after MI (Figure 6). These results suggest that JAM-A plays an important role in the prevention of neutrophil accumulation after MI as one of the CPC-derived paracrine factors.

Soluble JAM-A Mediates the Reduction of Infarct Size and Prevention of Left Ventricular Remodeling and Enhances Capillary Density

Next, we examined whether the beneficial effect of CPC+PM on the infarct size was mediated by JAM-A. When a mixture of JAM-A Fc protein and PM was injected into the infarct area, Masson's trichrome-stained myocardial images at 2 weeks after injection revealed that the infarct area of the heart treated with JAM-A+PM was smaller than that of PM-treated heart (Figure 7A, PM and JAM-A+PM). Average infarct area was $40.4\pm 3.0\%$ in PM-treated ($n=15$) and $25.0\pm 3.3\%$ in JAM-A-Fc-treated ($n=17$) hearts (PM versus JAM-A+PM; $P<0.01$; Figure 7B). When JAM-AsiCPC+PM was injected into the infarct area, Masson's trichrome-stained myocardial images at 2 weeks after injection revealed that the infarct area of JAM-AsiCPC+PM-treated heart was larger than that of CPC+PM-treated heart (Figure 7A, CPC+PM and JAM-AsiCPC+PM). Average infarct area was $26.1\pm 2.1\%$ in CPC+PM-treated ($n=16$) and $37.7\pm 3.3\%$ in JAM-AsiCPC+PM-treated ($n=15$) hearts (CPC+PM versus JAM-AsiCPC+PM; $P<0.05$; Figure 7B). Echocardiographic measurement of hearts at 2 weeks after transplantation revealed that both LVIDD and LVISD of JAM-A+PM- and CPC+PM-treated hearts were significantly smaller than those of the PM-treated group. LVISD of CPC+PM-treated hearts was significantly smaller than that of JAM-AsiCPC+PM-treated group. LVIDD of CPC+PM-treated hearts tends to be smaller than that of JAM-AsiCPC+PM-treated group (Table 4). These reductions

were associated with significantly greater value of percent FS of JAM-A+PM- and CPC+PM-treated hearts in comparison with that of the other 2 groups (Table 4). These findings suggest that JAM-A is one of the paracrine factors released from CPCs that plays an important role in attenuating cardiac remodeling and dysfunction at 2 weeks after MI through the prevention of neutrophils accumulation.

To examine the effect of JAM-A on neovascularization in post-MI hearts, we examined the number of vWF-positive capillaries in the ischemic area of PM- and JAM-A+PM-treated hearts. At 2 weeks after transplantation, immunohistochemical staining for vWF indicated that more vWF-positive capillaries exist in the border and infarct areas of the JAM-A+PM-treated heart in comparison with the PM-treated heart (Figure 7C). The number of vWF-positive capillaries was $90.0\pm 12/\text{mm}^2$ in PM-treated heart ($n=3$) and $141\pm 9.7/\text{mm}^2$ in JAM-A+PM-treated ($n=3$) hearts in the border area ($P<0.01$, Figure 7D). In the infarct area, the number of vWF-positive capillaries was $53.1\pm 4.2/\text{mm}^2$ in PM-treated heart ($n=3$) and $94.7\pm 24/\text{mm}^2$ in JAM-A+PM-treated ($n=3$) hearts in the border area ($P<0.05$; Figure 7E).

It has been reported that changes in fibroblastic properties during healing impact scar formation and that accumulation of the different collagens is connected with the impaired contractile function.¹⁵ We measured qualitative changes in collagen fibers by staining myocardial sections with picrosirius red at 2 weeks after MI. Sirius red polarization microscopy revealed that the treatment with JAM-A+PM decreased the ratio of green to yellow-orange fibers; however, the difference did not reach the statistical significant level against the other 3 groups (Figure 8).

Injection of CPC Prevents Reactive Oxygen Species Production and Early Inflammatory Response

Neutrophils have been implicated as a primary mechanisms underlying ischemic injury.¹⁶ Reactive oxygen species (ROS) production is one of the major processes that is involved in

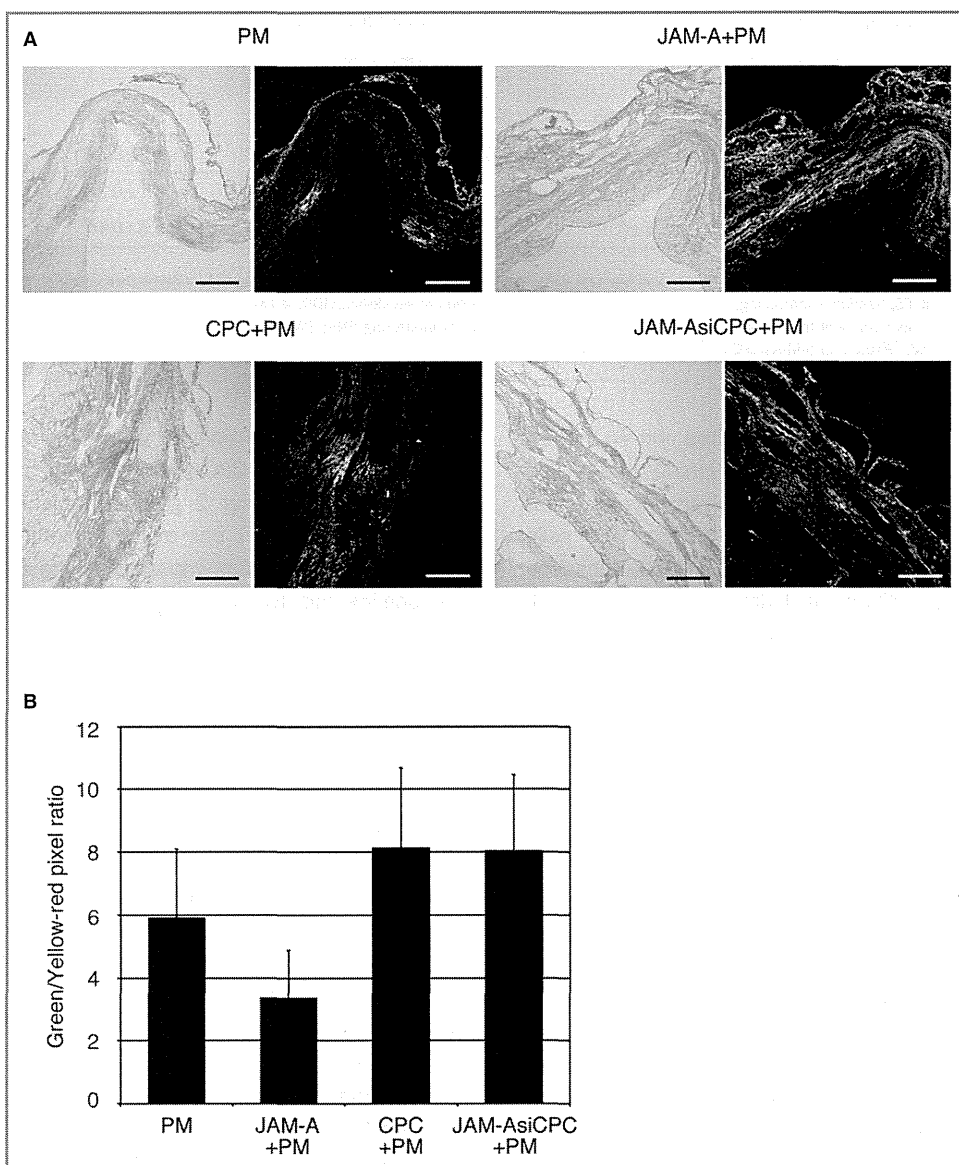


Figure 8. JAM-A does not affect scar maturation in infarcted myocardium. **A**, Representative Picro-Sirius red staining and polarization microscopy in PM-treated, JAM-A+PM-treated, CPC+PM-treated, and JAM-AsiCPC+PM-treated hearts. Bars are 200 μ m. **B**, Quantitative analysis of color component in infarct area. Vertical axis indicates the ratio of pixel number of green to that of yellow-red. A heart section at the level of the largest scar size was examined per mouse. An average of values obtained from 3 mice for each group was presented. For statistical analysis, 1-way ANOVA-Tukey-Kramer post hoc test was performed. CPC indicates cardiac progenitor cell; JAM-A, junctional adhesion molecule-A.

inducing tissue injury by neutrophils.^{17,18} To examine whether prevention of neutrophil accumulation by CPC+PM injection reduces ROS production, measurement of superoxide in myocardium submitted to MI was performed by using DHE. DHE fluorescence staining demonstrated that in the MI area, the DHE fluorescence intensity of the CPC+PM-treated group was lower than that of the PM-treated group (Figure 9A, PM and CPC+PM). The result of quantitative

analysis was shown in Figure 9B (PM: 2.68 ± 0.46 ; CPC+PM: 2.14 ± 0.20 , $P < 0.05$).

A variety of stimuli, including ROS generation, potentially stimulate induction of chemokines and proinflammatory cytokines. Several inducible chemokines have been reported to stimulate neutrophil chemotaxis and activation in the ischemic heart.¹⁹ Induction and release of the proinflammatory cytokines, such as IL-6, IL-1 β , and TNF α , have been

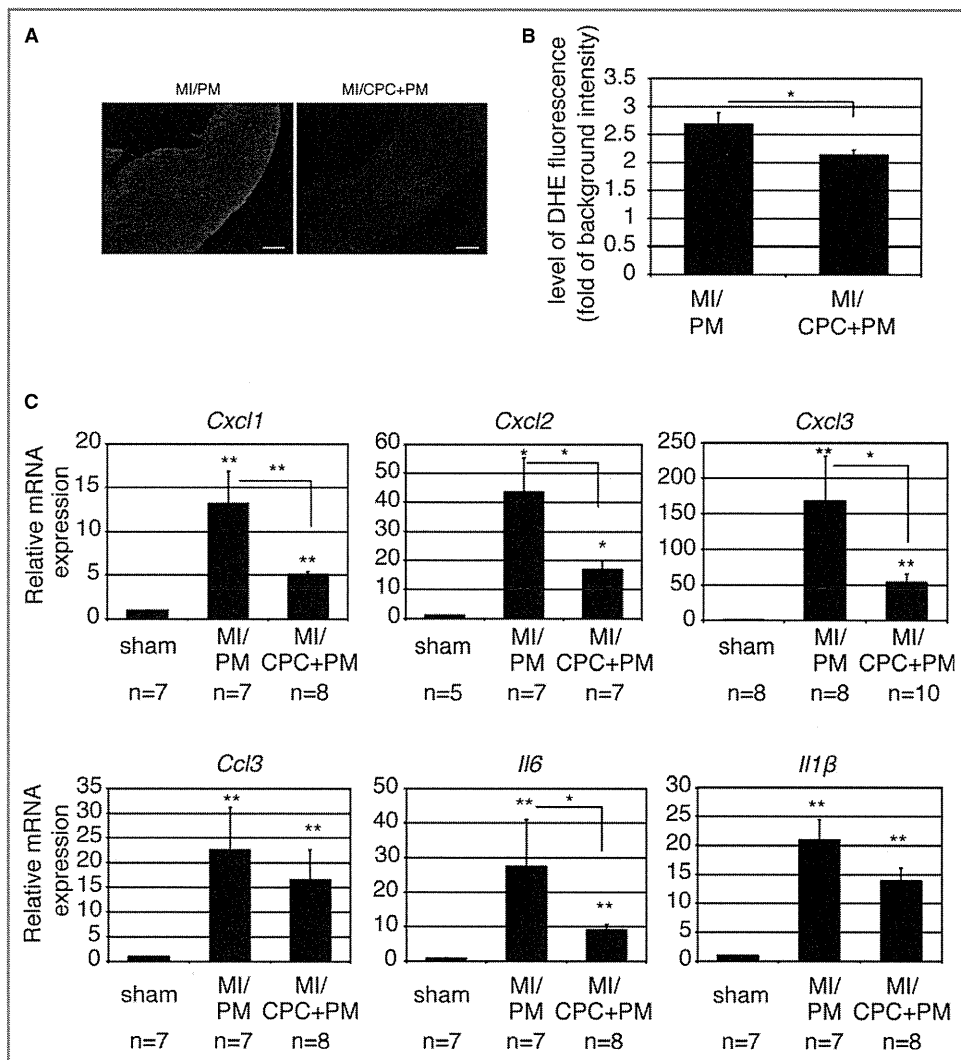


Figure 9. CPC transplantation attenuates ROS production and expression of various proinflammatory cytokines. **A**, Representative images from PM-treated and CPC+PM-treated hearts. At 1 day after MI, the heart sections were stained with dihydroethidium. Bars are 2 mm. **B**, Fluorescence intensity at infarct area. A heart section at the level of the largest infarct size was examined per mouse. An average of values obtained from 5 mice for each group was presented. For statistical analysis, Mann–Whitney *U* test was performed. Statistically significant differences between the 2 groups are shown by asterisks (**P*<0.05). **C**, Gene expression of various proinflammatory cytokines at 1 day after MI. Expression level was shown as fold changes relative to sham operated mouse using delta delta CT method. The number of mice examined was indicated below each graph. The Kruskal–Wallis test, followed by the Steel–Dwass test, was used for statistical analysis. Asterisks above individual columns indicate significant difference compared with sham. Asterisks above a line spanning 2 columns indicate significant difference between 2 groups (***P*<0.01 and **P*<0.05). CPC indicates cardiac progenitor cell; DHE, dihydroethidium; MI, myocardial infarction; ROS, reactive oxygen species.

demonstrated in the infarcted myocardium.²⁰ The results of quantitative real-time PCR revealed that expression of neutrophil chemoattractants and proinflammatory cytokines was upregulated at 24 hours after MI with the injection of PM; however, expression levels of *Cxcl1*, *Cxcl2*, *Cxcl3*, and *Il6* were significantly reduced in CPC+PM-treated MI hearts

(Figure 9C). Expression levels of *Ccl3* and *Il1β* also tended to be reduced in CPC+PM-treated MI hearts (Figure 9C). There was no significant difference in expression level of *Tnf-α* between PM- and CPC+PM-treated MI hearts (data not shown). The expression levels of the examined genes were decreased at 72 hours after MI, and no significant difference

was observed between PM-treated and CPC+PM-treated hearts (data not shown).

CPC-Derived Soluble JAM-A Reduces Neutrophil Motility

After adhesion and diapedesis through endothelial cells, emigrated neutrophils infiltrate the myocardial tissues toward neutrophil chemotactic factors. Therefore, we next examined whether CPC-derived soluble JAM-A reduces the motility of activated neutrophils. In response to the chemotactic factors, neutrophils attach to the substratum and polarize, leading to the establishment of a distinct leading edge (pseudopod) and tail (uropod).²¹ In order to maintain motility, migrating neutrophils must break adhesive contacts at the uropod and

establish new contacts at the pseudopod. When cell migration is impaired, the uropod remained tightly anchored to the substratum and often become flat or elongated tails.²² When neutrophils were preincubated with CPC CM, JAM-AsiCPC CM, CPC CM+anti-JAM-A antibody, or JAM-A Fc and then cultured on the fibronectin-coated dishes under the stimulation with WKYMV, actin immunofluorescence staining of neutrophils demonstrated that treatment with CPC CM or JAM-A Fc induced the formation of elongated (white arrowheads) or flattened (white arrow) uropods, whereas treatment with JAM-AsiCPC CM or CPC CM+anti-JAM-A antibody preserved short uropods (black arrowheads) as well as nontreated control neutrophils (Figure 10A). Treatment with CPC CM or JAM-A Fc decreased the percentage of neutrophils with uropod shorter than 5 μm and increased the percentage of neutrophils with

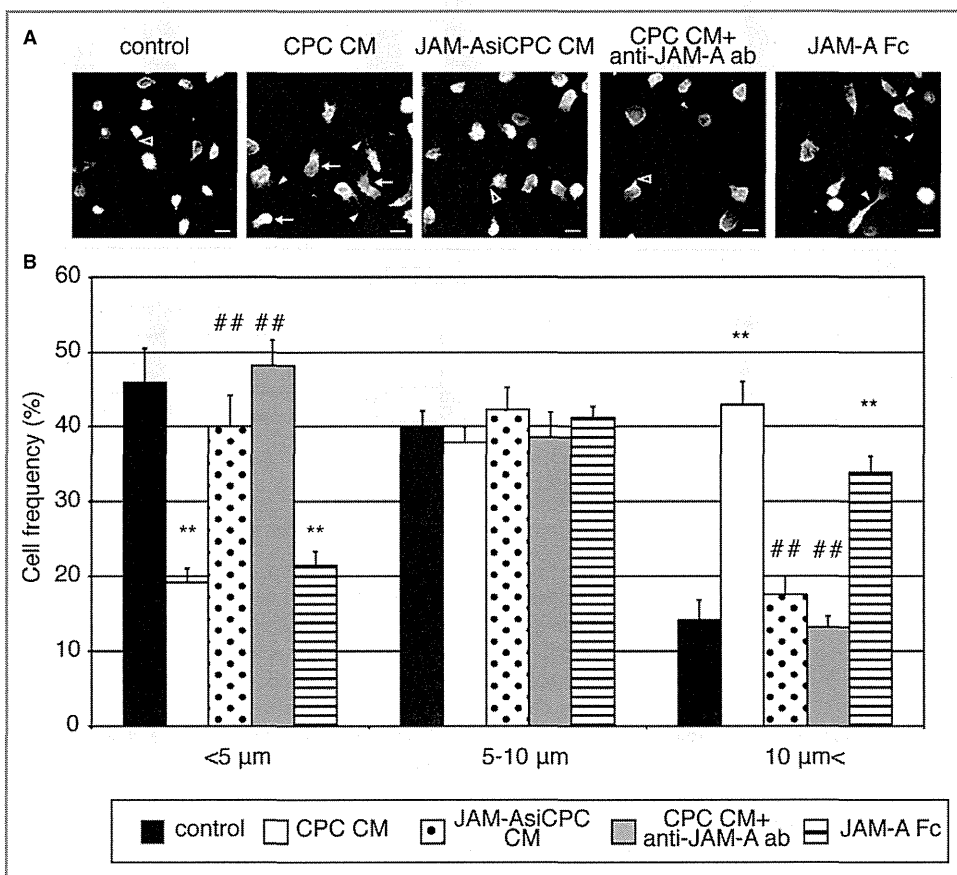


Figure 10. Soluble JAM-A derived from CPC alters the uropod length of neutrophils. A, Actin immunofluorescence staining of neutrophils pretreated with control medium, CPC CM, JAM-AsiCPC CM, CPC CM+anti-JAM-A antibody, or JAM-A Fc. Bars are 10 μm. B, The frequency of cells with different uropod length in 1 control and 4 treated groups. The graph shows the mean±SEM of 5 experiments. One-way ANOVA–Tukey–Kramer post hoc test was used for statistical analysis for different uropod length. Asterisks (** $P<0.01$) indicate significant differences between the treatment and control groups for different uropod length. Number signs (### $P<0.01$) indicate significant differences between the treatment and CPC CM groups for different uropod length. CM indicates conditioned medium; CPC, cardiac progenitor cell; JAM-A, junctional adhesion molecule-A.

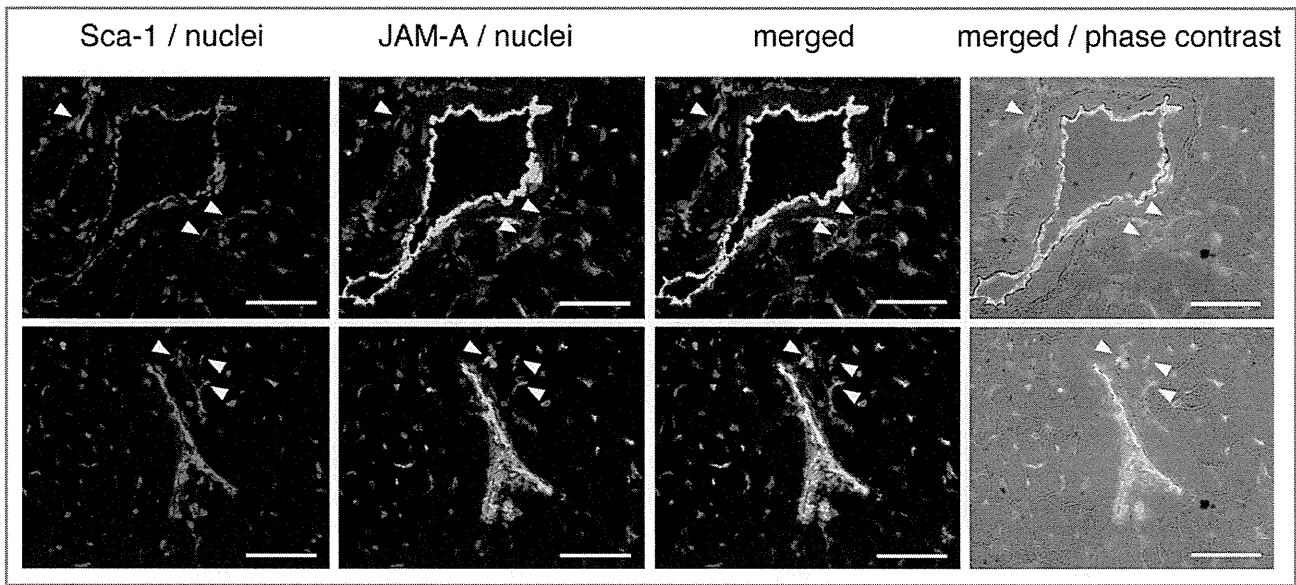


Figure 11. Immunohistochemical images of Sca-1 and JAM-A in normal mouse heart. Frozen sections were triple-stained with Sca-1 in red, JAM-A in green, and nuclei in blue. The images overlaid with phase contrast images are shown. White arrowheads indicate perivascular Sca-1–positive cells, which co-express JAM-A. Bars are 50 μ m. JAM-A indicates junctional adhesion molecule-A.

uropod longer than 10 μ m (Figure 10B). On the contrary, treatment with JAM-AsiCPC CM or CPC CM+anti-JAM-A antibody abolished the effects of CPC CM and JAM-A FC on uropod length, resulting in the distribution of uropod length similar to the control (Figure 10B). These findings suggest that soluble JAM-A released from injected CPC reduces the motility of neutrophils, preventing their infiltration into myocardial tissue, and ameliorates tissue damage to the infarct heart through the prevention of excessive inflammation.

Discussion

We previously reported that CPCs are most effective for cardiac repair in comparison with SMs, BMs, or AMCs.⁴ The dominance of CPC in part stems from not only their cardiomyogenic capacity but also unique paracrine factors. It has been reported that paracrine factors from transplanted cells are involved in various kinds of beneficial effects such as cytoprotection, angiogenesis, inhibition of fibrosis, and anti-inflammation.³ Here, we first reported that transplantation of CPC inhibited neutrophil infiltration after MI through the paracrine effect. We identified that JAM-A is exclusively secreted from CPCs and inhibited the emigration of neutrophils into myocardium, leading to reduction of oxidative stress and inflammatory response after infarction. In addition, we have shown that local delivery of JAM-A with self-assembling nanopeptides reduces cardiac remodeling after MI.

JAM-A is an immunoglobulin-like, PDZ binding domain containing transmembrane protein that is expressed in tight junction of endothelial and epithelial cells as well as leukocytes, including neutrophils, monocytes, and B- and T-lymphocytes.²³ JAM-A on endothelial cells associates through their extracellular domains with leukocyte function–associated antigen-1 and supports the adhesion and transendothelial migration of T cells and neutrophils. Although the mechanism by which JAM-A regulates leukocyte transendothelial migration is still unclear, Woodfin et al reported that JAM-A mediates neutrophil transmigration independent of other adhesion molecules such as intercellular adhesion molecule-2 and platelet endothelial cell adhesion molecule-1 through TNF α -mediated activation of leukocytes and endothelial cells *in vivo*.²⁴ Beside the membrane-tethered JAM-A, recently a soluble form of JAM-A and its anti-inflammatory effect have been identified. Koenen et al reported that soluble JAM-A is released from endothelial cells via proteolytic shedding by a disintegrin and metalloproteinases 10 and 17. This shedding process is enhanced by endothelial cell activation with TNF α and interferon- γ , resulting in inhibition of neutrophil transmigration by released soluble JAM-A.⁶ Thus, JAM-A and soluble JAM-A play important roles in regulating local inflammatory responses mediated by neutrophils.

The interface between neutrophils and endothelial cells appears to be a critical site of actions for soluble JAM-A, but that is not the case when CPCs or soluble JAM-A is directly delivered into myocardial tissue. Although a fraction of transplants may be excreted to the blood flow, it has been

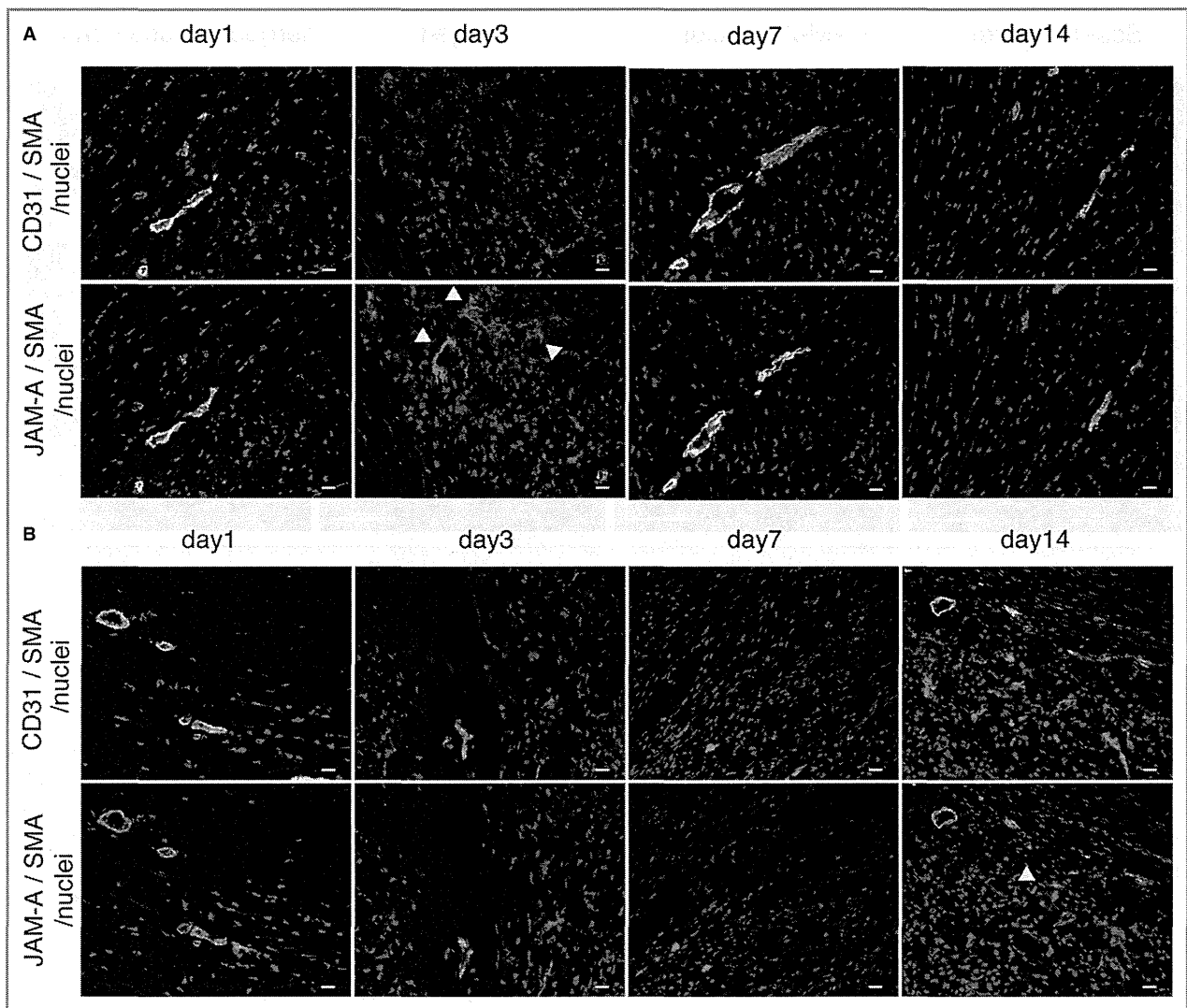


Figure 12. Time course of distribution and expression level of JAM-A following myocardial ischemia. A and B, Frozen sections obtained from border (A) and infarct area (B) 1, 3, 7, and 14 days following MI were stained with CD31 or JAM-A in red. The samples were costained with smooth muscle actin in green and nuclei in blue. As both CD31 and JAM-A antibody originated from rat IgG, a pair of serial sections was stained with CD31 and JAM-A, respectively. White arrowheads indicate CD31 negative nonendothelial JAM-A-positive cells. Bars are 20 μm . C and D, Semiquantitative immunofluorescence intensity of JAM-A and CD31 in border (C) and infarct area (D). One mouse was killed at each time point. Two adjacent sections were stained for CD31 and for JAMA separately. The values of immunofluorescence intensity obtained from at least 5 fields were examined. Two main effects and interaction effect were analyzed by using 2-factor factorial ANOVA (border area [C]; main effect of expressed protein: $P=0.27$, main effect of time: $P=6.5 \times 10^{-7}$, interaction effect: $P=0.75$, infarct area [D]; main effect of expressed protein: $P=0.0073$, main effect of time: $P=1.6 \times 10^{-9}$, interaction effect: $P=0.038$). The difference in the level of expressed proteins between time points was analyzed by 1-way ANOVA–Tukey–Kramer post hoc test. Asterisks and number signs above individual columns indicate significant difference compared with day 3 in C and with day 14 in (D) (** $P<0.01$, * $P<0.05$, ## $P<0.01$, and # $P<0.05$). We performed the experiment twice and similar results were obtained. JAM-A indicates junctional adhesion molecule-A; MI, myocardial infarction; SMA, smooth muscle actin.

reported that PM effectively retains the cells or proteins in the injected site.^{4,25} Therefore, the mechanism through which soluble JAM-A reduces the number of extravasated neutrophils is not simply due to the inhibition of transendothelial migration. Recently, Cera et al reported that on activated neutrophils, JAM-A is internalized in intracellular vesicles at

the leading edge and uropod where JAM-A codistributes with $\beta 1$ -integrin. Neutrophils derived from JAM-A-null mice were unable to correctly internalize and recycle $\beta 1$ -integrin during cell migration on chemotactic stimuli, and this caused impaired directional migration.²⁶ We have shown that treatment with soluble JAM-A reduces the motility of activated

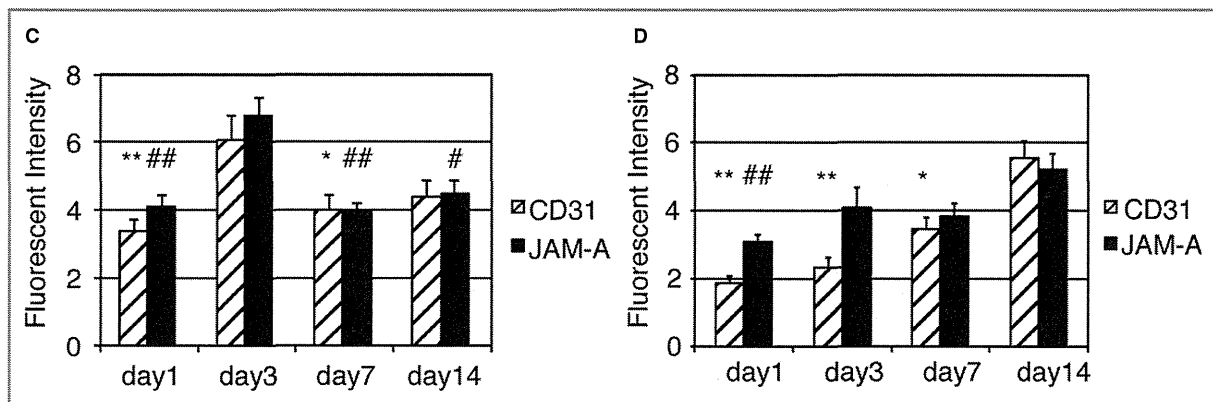


Figure 12. Continued.

neutrophils (Figure 10), suggesting that soluble JAM-A secreted from CPCs may bind to its homophilic or heterophilic counterparts of JAM-A or β 1-integrin on neutrophils, leading to failure of the colocalization of JAM-A and β 1-integrin and correct turnover of β 1-integrin on neutrophils when they migrate through the interstitial tissue of ischemic myocardium.

Immunohistochemical images of normal hearts revealed that JAM-A and Sca-1 are colocalized at perivascular cells as well as endothelial cells (Figure 11). The role of JAM-A-expressing perivascular cells has not been defined yet, but it is conceivable that the Sca-1-positive perivascular cells, in which Sca-1-positive CPCs are included, may control the fate of infiltrated leukocytes by secreting soluble JAM-A and contribute to the regulation of inflammatory response in the heart. It is interesting to know the amount and localization of endogenous JAM-A following myocardial ischemia. As shown in Figure 12, most of JAM-A was colocalized with CD31-positive endothelial cells of capillaries or those of smooth muscle actin-positive arterioles from day 1 to day 14 after MI (Figure 12A, border area; Figure 12B, infarct area). Semiquantitative analysis of fluorescent intensity revealed that the time courses of the expression level of JAM-A and CD31 were parallel and peaked at 3 days in the border area (Figure 12C). In the infarct area, the time course of the expression level of JAM-A transiently parted from that of CD31 at day 3 and subsequently both peaked at day 14 (Figure 12D). The reason for the time course difference between JAM-A and CD31 in the infarct area is unclear; however, taking into account the good colocalization of JAM-A with CD31-positive endothelial cells, the total amount of JAM-A in the ischemic area is mostly dependent on the level of vascularization after MI. CD31-negative nonendothelial JAM-A-positive cells were observed at day 3 in the border area and at day 14 in the infarct area (white arrowheads in Figure 12A and 12B). Although the identity

and the role of these interstitial JAM-A-positive cells are uncertain, these cells may contribute to an endogenous anti-inflammatory system in the acute and late phases of ischemia.

Neutrophils have been implicated as a primary mechanism underlying ischemic injury. The processes involved in inducing tissue injury by neutrophils include oxygen free radical generation, degranulation and release of proteases, and release of proinflammatory mediators.²⁷ After the hypoxic or mechanical stimulus is applied, cytokines such as TNF α and IL-6 are rapidly released in ischemic and border zones.^{28,29} The inflammatory cytokines induce the expression of endothelial adhesion molecules, such as selectin families, VCAM-1, and intercellular adhesion molecule-1, and promote leukocyte adhesion to the vascular endothelium and subsequent transendothelial migration.³⁰ Neutrophils stimulated by inflammatory cytokines produce superoxide anions and hydroxyl radicals in a respiratory burst.¹⁶ These oxygen free radicals promote the release of various kinds of proinflammatory chemokines from endothelial cells, cardiac fibroblasts, and other sources, leading to further enhancement of neutrophil adhesion and infiltration.^{27,31,32} Among these chemokines, CXC chemokines, including CXCL1, and CXCL2, play a critical role in basal and inflammatory neutrophil locomotion, trafficking, and activation.^{33,34} Recent studies revealed that neutrophils secrete CXCL1, CXCL2, CCL4, and CCL3 in response to a variety of stimulants, including lipopolysaccharides, zymosan, and substance P, thereby recruiting more neutrophils and activating themselves using the autocrine mechanisms of CXCL1 and CXCL2 secretion, and then attracting monocytes by using CCL4 and CCL3.³⁵ Activated monocytes have been reported to inhibit neutrophil apoptosis through granulocyte-macrophage colony-stimulating factor secretion.³⁶ McGettrick et al reported that neutrophils transmigrating through TNF α - or IL-1 β -treated HUVECs were strongly protected against apoptosis and that binding of β 2-integrins after transmigration

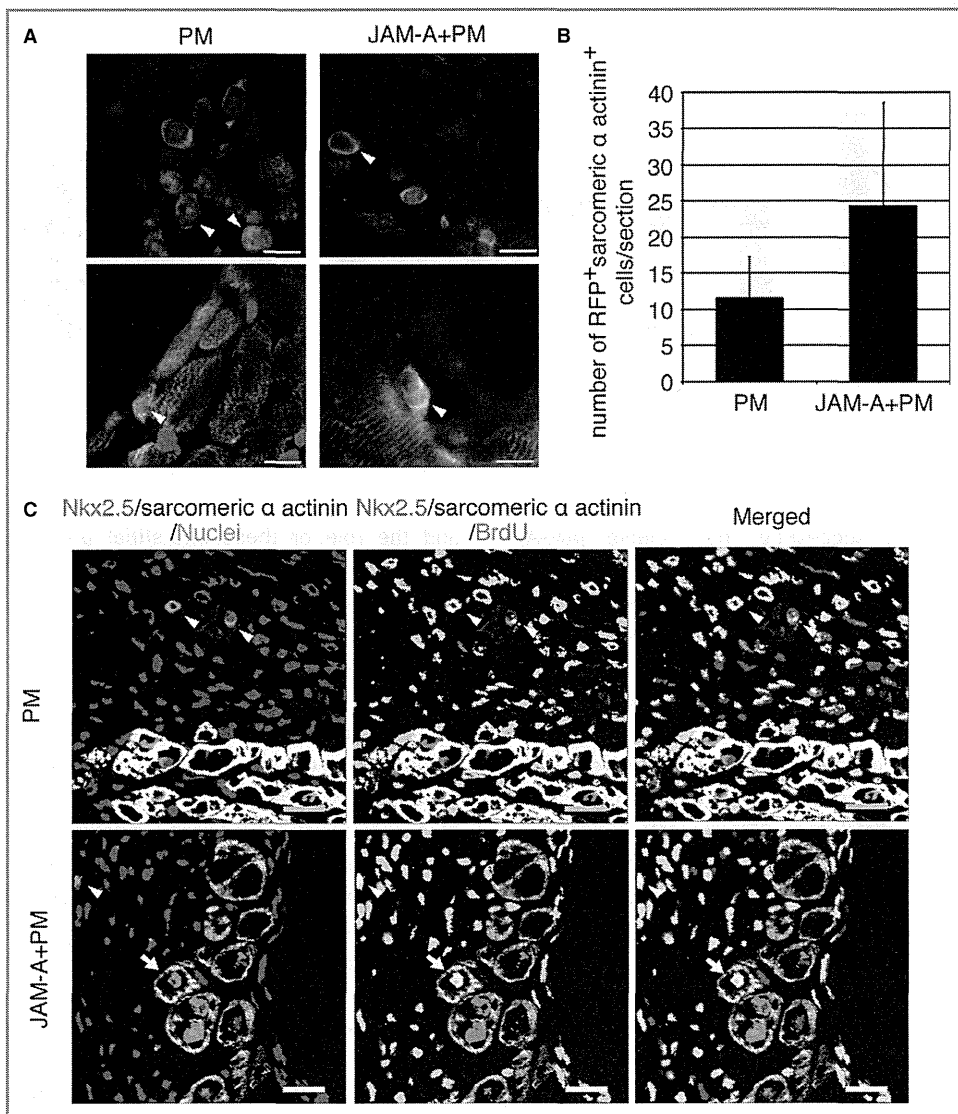


Figure 13. Cardiomyocyte-like differentiation of transplanted CPCs and proliferation of endogenous CPCs and cardiomyocytes in PM- and JAM-A+PM-treated hearts. **A**, Representative images of RFP (red) and sarcomeric α -actinin (green) double-positive cells (white arrowheads) in epicardial region (upper panels) and border area (lower panels). Nuclei were stained in blue. Bars are 10 μ m. **B**, Number of RFP and sarcomeric α -actinin double-positive cells per section of PM- and JAM-A+PM-treated hearts. An average of values obtained from 3 sections per mouse was analyzed: n=3 mice for PM- and n=4 mice for JAM-A+PM-treated group. Student *t* test was used for statistical analysis. **C**, Confocal images of BrdU-positive CPC (white arrowheads) and BrdU-positive cardiomyocytes (white arrows). Bars are 20 μ m. **D**, Frequency of BrdU-positive CPCs in total CPCs in PM- and JAM-A+PM-treated hearts. The whole area of LV in a section through the long axis of the heart was examined per mouse: n=3 mice for PM- and n=4 mice for JAM-A+PM-treated group. Student *t* test was used for statistical analysis. **E**, Frequency of BrdU-positive cardiomyocytes in PM- and JAM-A+PM-treated hearts. The whole area of LV in a section through the long axis of the heart was examined per mouse: n=3 mice per group. Student *t* test was used for statistical analysis. CPC indicates cardiac progenitor cell; JAM-A, junctional adhesion molecule-A; LV, left ventricle; RFP, red fluorescent protein.

was necessary for the survival signal for neutrophils, suggesting that an inflammatory condition during endothelial transmigration and integrin-mediated adhesion after transmigration is

essential for protection against neutrophil apoptosis.³⁷ In addition, it has been reported that the firm adhesion between cardiomyocytes and neutrophils through β 2- or α 4-integrins is

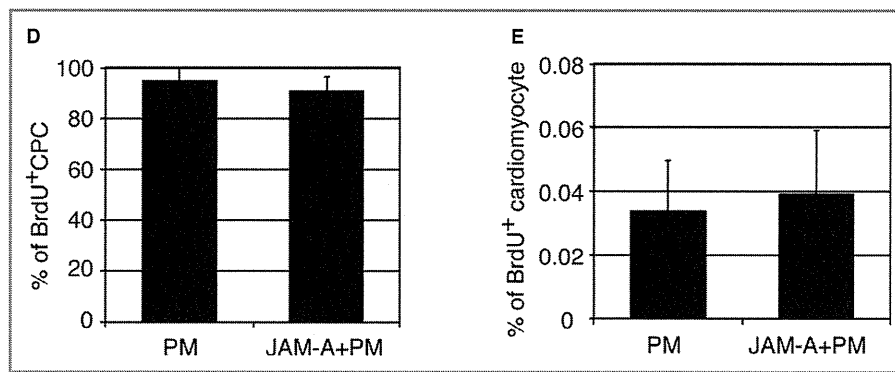


Figure 13. Continued.

required for both the release of toxic mediators including ROS and the subsequent injury and dysfunction.^{17,18} Therefore, reduction of ROS generation and downregulation of inflammatory chemokines expression may inhibit further neutrophil accumulation and survival, resulting in a reduction in neutrophil-derived toxic mediators and a decrease in the contact between emigrated neutrophils, which may lessen the tissue injury.

It has been reported that JAM-A is required for basic fibroblast growth factor–induced angiogenesis and is important in $\alpha V\beta 3$ -integrin–specific endothelial cell migration on vitronectin.^{38,39} Recently, Peddibhotla et al proposed a model of angiogenic signaling regulated by JAM-A and CD9, in which stimulation with basic fibroblast growth factor releases monomeric JAM-A from the JAM-A–CD9– $\alpha V\beta 3$ complex, subsequently inducing monomeric JAM-A to form homodimers that mediate mitogen-activated protein kinase activation.⁴⁰ Accordingly, antibodies against JAM-A, as well as genetic deletion of JAM-A, inhibited migration of endothelial cells. Considering the inhibitory effect of soluble JAM-A on neutrophil migration, it is possible that transplanted JAM-A may inhibit migration of endothelial cells and disturb angiogenesis. However, our data revealed that myocardial administration of soluble JAM-A enhances capillary density (Figure 7C through 7E). We suppose that reduction of neutrophil-derived ROS may prevent endothelial cells from massive death and maintain their function in the acute phase of MI or that endothelial the JAM-A– $\alpha V\beta 3$ complex may interact with soluble JAMA in a different way from neutrophil JAM-A/leukocyte function–associated antigen-1 complex.

We have explored the other mechanisms involved in the reduction of infarct size. It is generally accepted that thin collagen, such as collagen type III, is immature and deposited predominantly during early remodeling, while thick collagen (collagen type I) predominates during late remodeling stages and contributes to scar maturation.⁴¹ A sustained high ratio of green to yellow-red fibers means an excess of immature

collagen matrix and correlates with deterioration of cardiac remodeling. As shown in Figure 8, injection of JAM-A does not have a large effect on the composition of collagen fibers at least 2 weeks after MI.

The adult mammalian heart poses a limited capacity for regeneration, but recently it was reported that several factors can simulate cardiac regeneration after injury.⁴² We examined whether injection of JAM-A enhances cardiac regeneration through cardiac differentiation of transplanted CPCs, proliferation of endogenous CPCs, or cardiomyocyte division. When RFP-expressing CPCs were transplanted with PM or JAM-A+PM into MI heart, RFP and sarcomeric α -actinin double-positive cells were localized to epicardial lesion, where a mixture of CPCs and PM was overlaid (upper panels of Figure 13A). A few double-positive cells were localized to the border area (lower panels of Figure 13A). These double-positive cells were small and showed no or immature sarcomere structure. There was no significant difference in the number of double-positive cells per section between PM- and JAM-A+PM–treated groups (PM: 11.5 ± 5.7 [n=4]; JAM-A+PM: 24.3 ± 14 [n=3]; Figure 13B). We examined the frequency of BrdU-positive endogenous CPCs, which were identified as Nkx2.5 positive and sarcomeric α -actinin–negative cells (Figure 13C). There was no significant difference in the percentage of BrdU-positive CPCs in total CPCs between PM- and JAM-A+PM–treated mice (PM: $94.4 \pm 5.6\%$ [n=3]; JAM-A+PM: $90.9 \pm 5.5\%$ [n=4]; Figure 13D). The percentage of BrdU-positive cardiomyocytes in total cardiomyocytes did not show a significant difference between PM- and JAM-A+PM–treated mice (PM: $0.034 \pm 0.02\%$ [n=3]; JAM-A+PM: $0.039 \pm 0.02\%$ [n=3]; Figure 13E). These findings suggest that although a fraction of transplanted CPCs were engrafted and acquire cardiac phenotype, a large part of the beneficial effects of CPCs do not stem from cardiac regeneration in our model. In addition, JAM-A enhances neither the transdifferentiation of CPCs nor the intrinsic cardiac regeneration capacity after injury.

We have shown that transplantation of CPCs or soluble JAM-A protein, but not JAM-A knockdown CPCs, ameliorates cardiac remodeling and expansion of infarct size. This suggests that blocking neutrophil infiltration through the inactivation of JAM-A could be therapeutically valuable for the ischemic heart disease. Studies in models of myocardial ischemia and hepatic ischemia–reperfusion of JAM-A–deficient mouse have demonstrated that JAM-A deficiency in polymorphonuclear cells inhibits transendothelial migration of leukocytes but not their rolling and adhesion to endothelial cells.^{43,44} Although neutrophil infiltration was inhibited, increasing vascular adherent leukocytes results in the disturbance of blood flow and release of inflammatory mediators, consequently causing more tissue injury in comparison with wild-type.^{43,44} Recently, Lakshmi et al reported in a murine model of acute lung injury that JAM-A knockout and treatment with anti-JAM-A blocking antibody fail to reduce oxidative stress or cytokine and chemokine levels in whole lung and have no effect on capillary leakage and lung edema, presumably reflecting the histologically observed retention of neutrophils in lung tissue.⁴⁵ The plausible explanation of discordant results between previous reports and ours are as follows: systemic deletion of JAM-A or intravenous injection of anti-JAM-A blocking antibody may subject the circulating neutrophils to lose tuned balance between adhesion and transendothelial migration, whereas myocardial injection of CPCs or soluble JAM-A protein may specifically affect the extravasated neutrophils without retention of neutrophils in microvasculature in the heart.

A limitation of our study is a limited survival of transplanted CPCs. As shown in our previous report, the frequency of transplanted CPCs was only 0.21% at 7 days after transplantation.⁴ When cardiac function of PM- and CPC+PM–treated groups was examined at 4 weeks after myocardial infarction, both LVIDD and LVISD of CPC+PM–treated group were smaller and percent FS of the CPC+PM–treated group was higher than that of the PM-treated group, although the measured values did not reach statistical significance (Table 5). The infarct size was $42.2 \pm 2.6\%$ in the CPC+PM–treated group ($n=9$) and $49.1 \pm 4.8\%$ in the PM-treated group ($n=6$). Although the infarct size of the CPC+PM–treated group was

smaller than that of the PM-treated group, this finding did not reach statistical significance (Student *t* test). The reason for a lack of beneficial effects in a 4-week observation may stem from the poor survival of transplanted CPCs for a long period. However, we believe that good correlation between the survival time of transplanted CPCs and the phase of acute neutrophil accumulation indicates that JAM-A released from CPCs prevents deleterious effects derived from neutrophils during the acute phase of MI.

Although many researchers have reported the detrimental effects of infiltrating neutrophils and inflammatory mediators on cardiomyocytes in the infarcted heart, therapy directed to mitigate inflammatory processes has been, in general, unsuccessful in clinical practice.⁴⁶ The results of methylprednisolone trial have been controversial, in that some have demonstrated efficacy of the drug to limit extension of evolving MI, while other results have been deleterious.^{47,48} The results of a clinical trial demonstrated that an antibody to CD11/CD18 leukocyte integrin receptor did not reduce infarct size in patients who underwent primary angioplasty after MI.⁴⁹ Several methods for JAM-A inhibition, such as genetic inactivation, blocking antibody, and soluble recombinant proteins, prevent inflammatory reactions in meningitis, peritonitis, skin, and ischemic injury of heart and liver in animal models.^{6,50,51} However, the consequences of JAM-A targeting inhibition vary in different cell types and tissues, depending on the site (endothelium or leukocytes) and the mechanism (adhesion, diapedesis, or migration) of action. Systemic deletion of JAM-A gene or intravenous injection of JAM-A antibody caused retention of neutrophils on the vascular surface and, in some cases, aggregation in the capillaries. The permanence of neutrophils on the endothelial surface leads to the release of oxygen species and lytic enzymes, which aggravated tissue damage.^{43–45} Here, we have shown that local administration of soluble JAM-A into ischemic myocardium inhibits neutrophil emigration, probably without disturbing microcirculation, which suggests its usefulness for the clinical application. Although direct injection of JAM-A into myocardium during the acute ischemic phase is difficult to conduct, recent advances in nanoparticle-mediated drug deliver system may enable the transport of soluble JAM-A

Table 5. Echocardiographic Measurement of Hearts 4 Weeks After Transplantation

Parameter	n	HR, beats/min	SWT, mm	PWT, mm	LVIDD, mm	LVISD, mm	%FS
PM	4	689±19	0.17±0.01	0.49±0.09	6.1±0.48	5.7±0.59	7.7±3.0
CPC+PM	9	690±21	0.26±0.05	0.64±0.07	5.5±0.25	4.9±0.27	10.7±1.2

Statistical analysis was performed by using Student *t* test (PWT, LVIDD, and LVISD) or Mann–Whitney *U* test (HR, SWT and %FS). No statistical difference was observed between PM and CPC+PM in each parameter. FS indicates fractional shortening; HR, heart rate; LVIDD, left ventricular internal diastolic diameter; LVISD, left ventricular internal systolic diameter; PWT, posterior wall thickness; SWT, septal wall thickness.

across capillary endothelial cells by nanoparticle transcytosis following coronary injection.⁵² In addition, it has been reported that a small inhibitory peptide targeting the JAM-A- α L β 2 integrin interaction reduced leukocyte recruitment during postischemic inflammation in brain ischemia-reperfusion injury and reduced the lesion size.⁵³ Nanoparticles in which such a peptide inhibitor is encapsulated may be another choice for clinical anti-inflammatory strategy targeting JAM-A. The anti-inflammatory peptides secreted from cardiac dormant cells may become a new candidate for the treatment of cardiovascular disease through the prevention of excess inflammation.

Acknowledgments

The authors thank A. Furuyama and Y. Otsuki for their excellent technical assistance. We thank 3-D Matrix, Ltd for providing Puramatrix.

Sources of Funding

This work was supported by a Grant-in-Aid for Scientific Research, Developmental Scientific Research, and Scientific Research on Priority Areas from the Ministry of Education, Science, Sports, and Culture and the Takeda Science Foundation.

Disclosures

None.

References

- Rosenzweig A. Cardiac cell therapy-mixed results from mixed cells. *N Engl J Med*. 2006;355:1274–1277.
- Wollert KC, Drexler H. Cell therapy for the treatment of coronary heart disease: a critical appraisal. *Nat Rev Cardiol*. 2010;7:204–215.
- Gnecchi M, Zhang Z, Ni A, Dzau VJ. Paracrine mechanisms in adult stem cell signaling and therapy. *Circ Res*. 2008;103:1204–1219.
- Tokunaga M, Liu ML, Nagai T, Iwanaga K, Matsuura K, Takahashi T, Kanda M, Kondo N, Wang P, Naito AT, Komuro I. Implantation of cardiac progenitor cells using self-assembling peptide improves cardiac function after myocardial infarction. *J Mol Cell Cardiol*. 2010;49:972–983.
- Matsuura K, Honda A, Nagai T, Fukushima N, Iwanaga K, Tokunaga M, Shimizu T, Okano T, Kasanuki H, Hagiwara N, Komuro I. Transplantation of cardiac progenitor cells ameliorates cardiac dysfunction after myocardial infarction in mice. *J Clin Invest*. 2009;119:2204–2217.
- Koenen RR, Pruessmeyer J, Soehnlein O, Fraemohs L, Zerneck A, Schwarz N, Reiss K, Sarabi A, Lindbom L, Hackeng TM, Weber C, Ludwig A. Regulated release and functional modulation of junctional adhesion molecule A by disintegrin metalloproteinases. *Blood*. 2009;113:4799–4809.
- Matsuura K, Nagai T, Nishigaki N, Oyama T, Nishi J, Wada H, Sano M, Toko H, Akazawa H, Sato T, Nakaya H, Kasanuki H, Komuro I. Adult cardiac Sca-1-positive cells differentiate into beating cardiomyocytes. *J Biol Chem*. 2004;279:11384–11391.
- Planat-Bénard V, Menard C, André M, Puceat M, Perez A, Garcia-Verdugo JM, Penicaud L, Casteilla L. Spontaneous cardiomyocyte differentiation from adipose tissue stroma cells. *Circ Res*. 2004;94:223–229.
- Rando TA, Blau HM. Primary mouse myoblast purification, characterization, and transplantation for cell-mediated gene therapy. *J Cell Biol*. 1994;125:1275–1287.
- Matsuura K, Wada H, Nagai T, Iijima Y, Minamino T, Sano M, Akazawa H, Molkentin JD, Kasanuki H, Komuro I. Cardiomyocytes fuse with surrounding noncardiomyocytes and reenter the cell cycle. *J Cell Biol*. 2004;167:351–363.
- Allport JR, Ding HT, Ager A, Steeber DA, Tedder TF, Lucinskas FW. L-selectin shedding does not regulate human neutrophil attachment, rolling, or transmigration across human vascular endothelium invitro. *J Immunol*. 1997;158:4365–4372.
- Junqueira LC, Bignolas G, Brentani RR. Picrosirius staining plus polarization microscopy, a specific method for collagen detection in tissue sections. *Histochem J*. 1979;11:447–455.
- Rich L, Whittaker PB. Collagen and picrosirius red staining: a polarized light assessment of fibrillar hue and spatial distribution. *J Morphol Sci*. 2005;22:97–104.
- Seino Y, Ikeda U, Minezaki KK, Funayama H, Kasahara T, Konishi K, Shimada K. Expression of cytokine-induced neutrophil chemoattractant in rat cardiac myocytes. *J Mol Cell Cardiol*. 1995;27:2043–2051.
- Wei S, Chow LT, Shum IO, Qin L, Sanderson JE. Left and right ventricular collagen type I/III ratios and remodeling post-myocardial infarction. *J Card Fail*. 1999;5:117–126.
- Jordan JE, Zhao ZQ, Vinten-Johansen J. The role of neutrophils in myocardial ischemia-reperfusion injury. *Cardiovasc Res*. 1999;43:860–878.
- Entman ML, Youker K, Shoji T, Kukiella G, Shappell SB, Taylor AA, Smith CW. Neutrophil induced oxidative injury of cardiac myocytes. A compartmented system requiring CD11b/CD18-ICAM-1 adherence. *J Clin Invest*. 1992;90:1335–1345.
- Poon BY, Ward CA, Cooper CB, Giles WR, Burns AR, Kubus P. α 4-integrin mediates neutrophil-induced free radical injury to cardiac myocytes. *J Cell Biol*. 2001;152:857–866.
- Frangogiannis NG. The role of the chemokines in myocardial ischemia and reperfusion. *Curr Vasc Pharmacol*. 2004;2:163–174.
- Frangogiannis NG, Youker KA, Rossen RD, Gwechenberger M, Lindsey MH, Mendoza LH, Michael LH, Ballantyne CM, Smith CW, Entman ML. Cytokines and the microcirculation in ischemia and reperfusion. *J Mol Cell Cardiol*. 1998;30:2567–2576.
- Fais S, Malorni W. Leukocyte uropod formation and membrane/cytoskeleton linkage in immune interactions. *J Leukoc Biol*. 2003;73:556–563.
- Eddy RJ, Pierini LM, Matsumura F, Maxfield FR. Ca^{2+} -dependent myosin II activation is required for uropod retraction during neutrophil migration. *J Cell Sci*. 2000;113:1287–1298.
- Severson EA, Parkos CA. Mechanisms of outside-in signaling at the tight junction by junctional adhesion molecule A. *Ann N Y Acad Sci*. 2009;1165:10–18.
- Woodfin A, Voisin MB, Imhof BA, Dejana E, Engelhardt B, Nourshargh S. Endothelial cell activation leads to neutrophil transmigration as supported by the sequential roles of ICAM-2, JAM-A, and PECAM-1. *Blood*. 2009;113:6246–6257.
- Gelain F, Unsworth LD, Zhang S. Slow and sustained release of active cytokines from self-assembling peptide scaffolds. *J Control Release*. 2010;145:231–239.
- Cera MR, Fabbrì M, Molendini C, Corada M, Orsenigo F, Rehberg M, Reichel CA, Krombach F, Pardi R, Dejana E. JAM-A promotes neutrophil chemotaxis by controlling integrin internalization and recycling. *J Cell Sci*. 2009;122:268–277.
- Frangogiannis NG, Smith CW, Entman ML. The inflammatory response in myocardial infarction. *Cardiovasc Res*. 2002;53:31–47.
- Irwin MW, Mak S, Mann DL, Qu R, Penninger JM, Yan A, Dawood F, Wen WH, Shou Z, Liu P. Tissue expression and immunolocalization of tumour necrosis factor- α in post infarction-dysfunctional myocardium. *Circulation*. 1999;99:1492–1498.
- Ono K, Matsumori A, Shioi T, Furukawa Y, Sasayama S. Cytokine gene expression after myocardial infarction in rat hearts: possible implication in left ventricular remodeling. *Circulation*. 1998;98:149–156.
- Zhang J, Alcaide P, Liu L, Sun J, He A, Lucinskas FW, Shi GP. Regulation of endothelial cell adhesion molecule expression by mast cells, macrophages, and neutrophils. *PLoS One*. 2011;6:e14525.
- Lewis MS, Whatley RE, Cain P, McIntyre TM, Prescott SM, Zimmerman GA. Hydrogen peroxide stimulates the synthesis of platelet-activating factor by endothelium and induces endothelial cell-dependent neutrophil adhesion. *J Clin Invest*. 1988;82:2045–2055.
- Long CS. The role of interleukin-1 in the failing heart. *Heart Fail Rev*. 2001;6:81–94.
- Gerard C, Rollins BJ. Chemokines and disease. *Nat Immunol*. 2001;2:108–115.

34. Moser B, Loetscher P. Lymphocyte traffic control by chemokines. *Nat Immunol.* 2001;2:123–128.
35. Kobayashi Y. The role of chemokines in neutrophil biology. *Front Biosci.* 2008;13:2400–2407.
36. Klein JB, Rane MJ, Scherzer JA, Coxon PY, Kettritz R, Mathiesen JM, Buridi A, McLeish KR. Granulocyte-macrophage colonystimulating factor delays neutrophil constitutive apoptosis through phosphoinositide 3-kinase and extracellular signal-regulated kinase pathways. *J Immunol.* 2000;164:4286–4291.
37. McGettrick HM, Lord JM, Wang KO, Rainger GE, Buckley CD, Nash GB. Chemokine- and adhesion-dependent survival of neutrophils after transmigration through cytokine-stimulated endothelium. *J Leukoc Biol.* 2006;79:779–788.
38. Naik MU, Vuppalanchi D, Naik UP. Essential role of junctional adhesion molecule-1 in basic fibroblast growth factor-induced endothelial cell migration. *Arterioscler Thromb Vasc Biol.* 2003;23:2165–2171.
39. Naik MU, Naik UP. Junctional adhesion molecule-A-induced endothelial cell migration on vitronectin is integrin $\alpha V\beta 3$ specific. *J Cell Sci.* 2006;119:490–499.
40. Peddibhotla SS, Brinkmann BF, Kummer D, Tuncay H, Nakayama M, Adams RH, Gerke V, Ebneth K. Tetraspanin CD9 links junctional adhesion molecule-A to $\alpha V\beta 3$ integrin to mediate basic fibroblast growth factor-specific angiogenic signaling. *Mol Biol Cell.* 2013;24:933–944.
41. Whittaker P, Kloner RA, Boughner DR, Pickering JG. Quantitative assessment of myocardial collagen with picrosirius red staining and circularly polarized light. *Basic Res Cardiol.* 1994;89:397–410.
42. Kikuchi K, Poss KD. Cardiac regenerative capacity and mechanisms. *Annu Rev Cell Dev Biol.* 2012;28:719–741.
43. Khandoga A, Kessler JS, Meissner H, Hanschen M, Corada M, Motoike T, Enders G, Dejana E, Krombach F. Junctional adhesion molecule-A deficiency increases hepatic ischemia-reperfusion injury despite reduction of neutrophil transendothelial migration. *Blood.* 2005;106:725–733.
44. Corada M, Chimenti S, Cera MR, Vinci M, Salio M, Fiordaliso F, De Angelis N, Villa A, Bossi M, Staszewsky LI, Vecchi A, Parazzoli D, Motoike T, Latini R, Dejana E. Junctional adhesion molecule-A-deficient polymorphonuclear cells show reduced diapedesis in peritonitis and heart ischemia-reperfusion injury. *Proc Natl Acad Sci USA.* 2005;102:10634–10639.
45. Lakshmi SP, Reddy AT, Naik MU, Naik UP, Reddy RC. Effects of JAM-A deficiency or blocking antibodies on neutrophil migration and lung injury in a murine model of acute lung injury. *Am J Physiol Lung Cell Mol Physiol.* 2012;303:L758–L766.
46. Seropian IM, Toldo S, Van Tassel BW, Abbate A. Anti-inflammatory strategies for ventricular remodeling following ST-segment elevation acute myocardial infarction. *J Am Coll Cardiol.* 2014;63:1593–1603.
47. LeGal YM, Morrissey LL. Methylprednisolone interventions in myocardial infarction: a controversial subject. *Can J Cardiol.* 1990;6:405–410.
48. Roberts R, DeMello V, Sobel BE. Deleterious effects of methylprednisolone in patients with myocardial infarction. *Circulation.* 1976;53:1204–1206.
49. Faxon DP, Gibbons RJ, Chronos NA, Gurbel PA, Sheehan F. The effect of blockade of the CD11/CD18 integrin receptor on infarct size in patients with acute myocardial infarction treated with direct angioplasty: the results of the HALTMI study. *J Am Coll Cardiol.* 2002;40:1199–1204.
50. Nourshargh S, Krombach F, Dejana E. The role of JAM-A and PECAM-1 in modulating leukocyte infiltration in inflamed and ischemic tissues. *J Leukoc Biol.* 2006;80:714–718.
51. Weber C, Fraemohs L, Dejana E. The role of junctional adhesion molecules in vascular inflammation. *Nat Rev Immunol.* 2007;7:467–477.
52. Kreuter J. Drug delivery to the central nervous system by polymeric nanoparticles: what do we know? *Adv Drug Deliv Rev.* 2014;71:2–14.
53. Sladojevic N, Stamatovic SM, Keep RF, Grailer JJ, Sarma JV, Ward PA, Andjelkovic AV. Inhibition of junctional adhesion molecule-A/LFA interaction attenuates leukocyte trafficking and inflammation in brain ischemia/reperfusion injury. *Neurobiol Dis.* 2014;67:57–70.

Anti-Inflammatory Peptides From Cardiac Progenitors Ameliorate Dysfunction After Myocardial Infarction

Mei-Lan Liu, Toshio Nagai, Masakuni Tokunaga, Koji Iwanaga, Katsuhisa Matsuura, Toshinao Takahashi, Masato Kanda, Naomichi Kondo, Atsuhiko T. Naito, Issei Komuro and Yoshio Kobayashi

J Am Heart Assoc. 2014;3:e001101; originally published December 2, 2014;

doi: 10.1161/JAHA.114.001101

The *Journal of the American Heart Association* is published by the American Heart Association, 7272 Greenville Avenue, Dallas, TX 75231

Online ISSN: 2047-9980

The online version of this article, along with updated information and services, is located on the World Wide Web at:

<http://jaha.ahajournals.org/content/3/6/e001101>

Subscriptions, Permissions, and Reprints: The *Journal of the American Heart Association* is an online only Open Access publication. Visit the Journal at <http://jaha.ahajournals.org> for more information.

Trans-ancestry mutational landscape of hepatocellular carcinoma genomes

Yasushi Totoki^{1,14}, Kenji Tatsuno^{2,14}, Kyle R Covington^{3,14}, Hiroki Ueda², Chad J Creighton^{3,4}, Mamoru Kato¹, Shingo Tsuji², Lawrence A Donehower⁵, Betty L Slagle⁵, Hiromi Nakamura¹, Shogo Yamamoto², Eve Shinbrot³, Natsuko Hama¹, Megan Lehmkuhl³, Fumie Hosoda¹, Yasuhito Arai¹, Kim Walker³, Mahmoud Dahdouli³, Kengo Gotoh², Genta Nagae², Marie-Claude Gingras³, Donna M Muzny³, Hidenori Ojima⁶, Kazuaki Shimada⁷, Yutaka Midorikawa⁸, John A Goss⁹, Ronald Cotton⁹, Akimasa Hayashi^{2,10}, Junji Shibahara¹⁰, Shumpei Ishikawa¹⁰, Jacfranz Guiteau⁹, Mariko Tanaka¹⁰, Tomoko Urushidate¹, Shoko Ohashi¹, Naoko Okada¹, Harsha Doddapaneni³, Min Wang³, Yiming Zhu³, Huyen Dinh³, Takuji Okusaka¹¹, Norihiro Kokudo¹², Tomoo Kosuge⁷, Tadatoshi Takayama⁸, Masashi Fukayama¹⁰, Richard A Gibbs³, David A Wheeler³, Hiroyuki Aburatani² & Tatsuhiko Shibata^{1,13}

Diverse epidemiological factors are associated with hepatocellular carcinoma (HCC) prevalence in different populations. However, the global landscape of the genetic changes in HCC genomes underpinning different epidemiological and ancestral backgrounds still remains uncharted. Here a collection of data from 503 liver cancer genomes from different populations uncovered 30 candidate driver genes and 11 core pathway modules. Furthermore, a collaboration of two large-scale cancer genome projects comparatively analyzed the trans-ancestry substitution signatures in 608 liver cancer cases and identified unique mutational signatures that predominantly contribute to Asian cases. This work elucidates previously unexplored ancestry-associated mutational processes in HCC development. A combination of hotspot *TERT* promoter mutation, *TERT* focal amplification and viral genome integration occurs in more than 68% of cases, implicating *TERT* as a central and ancestry-independent node of hepatocarcinogenesis. Newly identified alterations in genes encoding metabolic enzymes, chromatin remodelers and a high proportion of mTOR pathway activations offer potential therapeutic and diagnostic opportunities.

HCC is the third leading cause of cancer deaths worldwide^{1,2}. Epidemiologically, the incidence of HCC shows marked variance across geographical regions and ancestry groups and between the sexes³. HCC incidence predominates in East Asia and Africa, and rapid increases in prevalence have occurred in Western countries². Multiple etiological cofactors are associated with liver cancer, and their contributions might additionally differ according to ancestry. Hepatitis B virus (HBV) infection is dominant in East Asia and Africa, whereas hepatitis C virus (HCV) infection among HCC cases is frequent in Japan. Aflatoxin B1 exposure is a strong risk factor of HCC in China and Africa, whereas alcohol intake is a major etiological factor for HCC in Western countries^{3–5}. The average male/female ratio for HCC incidence is greater than two, which could be owing to different environmental exposures or hormone levels⁶. Overlapping but partially distinctive epidemiological backgrounds, such as liver

fluke infection, were associated with intrahepatic cholangiocarcinoma (IHCC), another type of liver cancer⁵. Here we conducted the first trans-ancestry HCC genome sequencing research under the umbrella of the International Cancer Genome Consortium (ICGC)⁷ and The Cancer Genome Atlas (TCGA)⁸. Thus far, this study represents the largest genomic profiling of liver cancers (608 cases) and compares ancestry groups (Japanese, Asian and European) with distinctive etiological cofactors. This genome data set also uncovers an extensive landscape of driver genetic alterations in HCC.

RESULTS

Whole-exome and oncovirome sequencing of liver cancers

As an ICGC liver cancer project, we collected 503 pairs (413 cases in the Japanese cohort and 90 cases in the US cohort) of liver cancers (488 HCC and 15 IHCC) and matched non-cancerous liver tissues

¹Division of Cancer Genomics, National Cancer Center Research Institute, Tokyo, Japan. ²Genome Science Division, Research Center for Advanced Science and Technology, The University of Tokyo, Tokyo, Japan. ³Human Genome Sequencing Center, Baylor College of Medicine, Houston, Texas, USA. ⁴Department of Medicine, Baylor College of Medicine, Houston, Texas, USA. ⁵Department of Molecular Virology and Microbiology, Baylor College of Medicine, Houston, Texas, USA. ⁶Division of Molecular Pathology, National Cancer Center Research Institute, Tokyo, Japan. ⁷Hepatobiliary and Pancreatic Surgery Division, National Cancer Center Hospital, Tokyo, Japan. ⁸Department of Digestive Surgery, Nihon University School of Medicine, Tokyo, Japan. ⁹Department of Surgery, Baylor College of Medicine, Houston, Texas, USA. ¹⁰Department of Pathology, Graduate School of Medicine, The University of Tokyo, Tokyo, Japan. ¹¹Hepatobiliary and Pancreatic Oncology Division, National Cancer Center Hospital, Tokyo, Japan. ¹²Hepato-Biliary-Pancreatic Surgery Division, Department of Surgery, Graduate School of Medicine, The University of Tokyo, Tokyo, Japan. ¹³Laboratory of Molecular Medicine, Human Genome Center, Institute of Medical Science, The University of Tokyo, Tokyo, Japan. ¹⁴These authors contributed equally to this work. Correspondence should be addressed to D.A.W. (wheeler@bcm.edu), H.A. (haburata-ky@umin.ac.jp) or T.S. (tashibat@ncc.go.jp).

Received 31 December 2013; accepted 3 October 2014; published online 2 November 2014; doi:10.1038/ng.3126